

## Supporting Information

# Reclamation and reuse of graphite from electric vehicle lithium-ion battery anodes via water delamination.

Alexander T. Sargent<sup>\*a,b</sup>, Zoë Henderson<sup>c</sup>, Alex S. Walton<sup>c</sup>, Ben F. Spencer<sup>d</sup>, Luke Sweeney<sup>a,b</sup>, Wendy R. Flavell<sup>e</sup>, Paul A. Anderson<sup>a,b</sup>, Emma Kendrick<sup>b,f</sup>, Peter R. Slater<sup>\*a,b</sup>, and Phoebe K. Allan<sup>\*a,b</sup>

- 
- a. School of Chemistry, University of Birmingham, Birmingham, B15 2TT, UK.*
  - b. The Faraday Institution, Quad One, Harwell Science and Innovation Campus, Didcot, UK.*
  - c. Department of Chemistry and Photon Science Institute, University of Manchester, Oxford Road, Manchester, UK.*
  - d. Department of Materials and Henry Royce Institute, University of Manchester, Oxford Road, Manchester, UK.*
  - e. Department of Physics and Astronomy, Henry Royce Institute, and Photon Science Institute, University of Manchester, Oxford Road, Manchester, UK.*
  - f. School of Metallurgy and Materials, University of Birmingham, Birmingham, B15 2TT, UK.*

Email of correspondence: [axs1256@student.bham.ac.uk](mailto:axs1256@student.bham.ac.uk), [p.r.slater@bham.ac.uk](mailto:p.r.slater@bham.ac.uk), [p.allan@bham.ac.uk](mailto:p.allan@bham.ac.uk).



Table S1: The constraints used within casaXPS for the assigned peaks for Fig. 1. Similar peak positions found in literature are also shown. Literature positions following “~” were obtained from the figures binding energy axis as the binding energy value were not stated. Literature reference numbers used within the table refer to references given on the right.

	Peak position constraint (eV)	FWHM constraint (eV)	Values found in literature (eV)
LiG	283.5-281.0	0 to 2	282 [1] 281.9-282.0 [2]
C-C/C-H	285-284.6	0 to 2	284.8 [3] [4] 284.4 [2]
C-O	286.2-285.8	Same as C-C/C-H	285 [3] 286 [5] 285.5 [4] 286.1-286.2 [2]
C=O	287.5-285.9	Same as C-C/C-H	286.5 [7] ~286.5 [5] 288.7 [2]
O-C=O	288.7-288.3	Same as C-C/C-H	~288.9 [7] ~288.5 [5]
CO <sub>3</sub> -2	290.2-289.8	Same as C-C/C-H	~290 [5] 292.9-293.3 [2]
Fluorocarbons	294-290	Same as C-C/C-H	287.2- 294.2 [6]
LiPF <sub>6</sub>	692.0-676.2	Same as LiyPFx/LiPFx(OR)y	~688 [7]
LiyPFx/LiPFx(OR)y	692.0-676.2	0 to 2	~686.6 [7] 687.0-687.5 [2]
LiF	692.0-676.2	Same as LiyPFx/LiPFx(OR)y	~685 [7] 684.6 eV [1] 684.1-684.9 [2]

1. S. Malmgren, K. Ciosek, R. Lindblad, S. Plogmaker, J. Kühn, H. Rensmo, K. Edström and M. Hahlin, *Electrochim. Acta*, 2013, **105**, 83–91.
2. S. Malmgren, K. Ciosek, M. Hahlin, T. Gustafsson, M. Gorgoi, H. Rensmo and K. Edström, *Electrochim. Acta*, 2013, **97**, 23–32.
3. R. Blume, D. Rosenthal, J. P. Tessonier, H. Li, A. Knop-Gericke and R. Schlögl, *ChemCatChem*, 2015, **7**, 2871–2881.
4. T. S. Pathan, M. Rashid, M. Walker, W. D. Widanage and E. Kendrick, *J. Phys. Energy*, 2019, **1**, 044003.
5. S. Jiao, X. Ren, R. Cao, M. H. Engelhard, Y. Liu, D. Hu, D. Mei, J. Zheng, W. Zhao, Q. Li, N. Liu, B. D. Adams, C. Ma, J. Liu, J. G. Zhang and W. Xu, *Nat. energy*, 2018, **3**, 739–746.
6. J. Piwowarczyk, R. Jedrzejewski, D. Moszynski, K. Kwiatkowski, A. Niemczyk and J. Baranowska, *Polymers (Basel)*, 2019, **11**, 1629.
7. L. Somerville, J. Bareño, P. Jennings, A. McGordon, C. Lyness and I. Bloom, *Electrochim. Acta*, 2016, **206**, 70–76.

Table S2: Positions and FWHM of each peak used for the carbon 1s and fluorine 1s fitting for Fig. 1.

		Carbon 1s Peak Fittings												Fluorine 1s Peak Fittings							
		LiG		C-C/C-H		C-O		C=O		O-C=O		CO <sub>3</sub> <sup>2-</sup>		Fluorocarbons		LiPF <sub>6</sub>		LiyPFx/LiPFx(OR)y		LiF	
		Peak Position (eV)	FWHM (eV)	Peak Position (eV)	FWHM (eV)	Peak Position (eV)	FWHM (eV)	Peak Position (eV)	FWHM (eV)	Peak Position (eV)	FWHM (eV)	Peak Position (eV)	FWHM (eV)	Peak Position (eV)	FWHM (eV)	Peak Position (eV)	FWHM (eV)	Peak Position (eV)	FWHM (eV)	Peak Position (eV)	FWHM (eV)
QCR	XPS	281.2	0.9	284.9	1.2	285.8	1.2	287	1.2	288.7	1.2	290.2	1.2	-	-	688.6	1.8	686.9	1.8	685.2	1.8
	HAXPES	282	0.3	284.7	1.4	285.8	1.4	286.8	1.4	288.5	1.4	290.2	1.4	-	-	-	-	687.1	1.9	684.9	1.9
QCR II	XPS	283.2	0.8	284.9	1.3	286.2	1.3	287	1.3	288.7	1.3	290	1.3	-	-	-	-	687.6	1.6	685	1.6
	HAXPES	283.3	1	284.7	1.6	286	1.6	287	1.6	288.6	1.6	290.1	1.6	-	-	-	-	687.5	1.8	684.9	1.8
EoL	XPS	283.1	0.6	284.7	1.5	286.1	1.5	287	1.5	288.7	1.5	289.8	1.5	-	-	-	-	686.8	1.9	685	1.9
	HAXPES	283.1	1.3	284.6	1.5	285.9	1.5	286.8	1.5	288.7	1.5	289.8	1.5	-	-	-	-	686.7	2	684.7	2
EoL II	XPS	282.9	1.6	284.9	1.4	286.1	1.4	287	1.4	288.5	1.4	289.9	1.4	-	-	687.9	1.5	686.8	1.5	685.1	1.5
	HAXPES	282.5	1	284.7	1.7	286.1	1.7	286.8	1.7	288.7	1.7	289.9	1.7	-	-	-	-	687.1	1.9	685	1.9
EoL III	XPS	282.7	0.6	285	1.5	286.2	1.5	287.1	1.5	288.7	1.5	287.1	1.5	291.5	1.5	688.6	1.8	686.9	1.8	685.2	1.8
	HAXPES	282.8	1.9	284.6	1.8	282.8	1.8	287.2	1.8	288.7	1.8	287.2	1.8	-	-	687.3	1.7	686	1.7	684.6	1.7

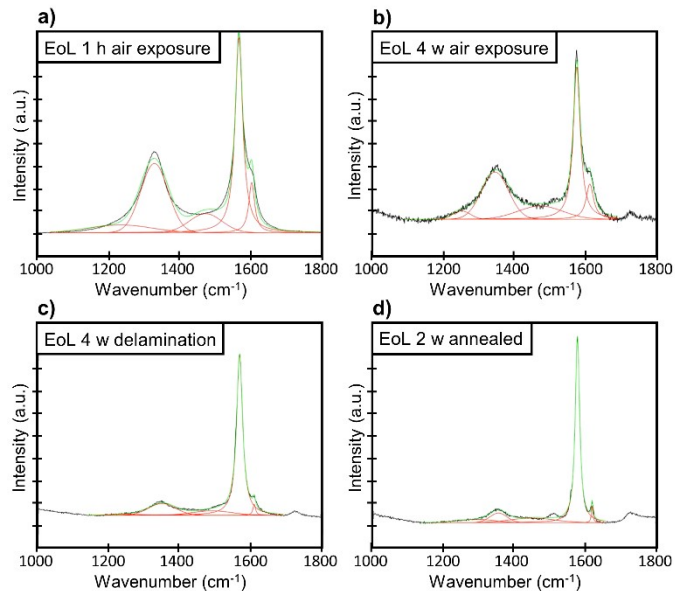


Fig. S1: Examples of the fittings applied to the graphitic Raman region ( $1200\text{--}1700\text{ cm}^{-1}$ ) for EoL at different stages of processing. Here 5 peaks were used after a linear background fit, 3 Voigt shaped peaks for D4 ( $1150\text{--}1310\text{ cm}^{-1}$ ), D ( $1320\text{--}1380\text{ cm}^{-1}$ ) and D3 ( $1350\text{--}1450\text{ cm}^{-1}$ ) and 2 Lorentzian shaped peaks for the G ( $1525\text{--}1590\text{ cm}^{-1}$ ) and D' ( $1590\text{--}1635\text{ cm}^{-1}$ ). a) EoL exposed to air for 1 hour b) EoL exposed to air for 4 weeks c) EoL exposed to air for 4 weeks then delaminated via submersion into water d) EoL delaminated after 2 weeks of air exposure then annealed to  $500\text{ }^{\circ}\text{C}$  for 1 hour.

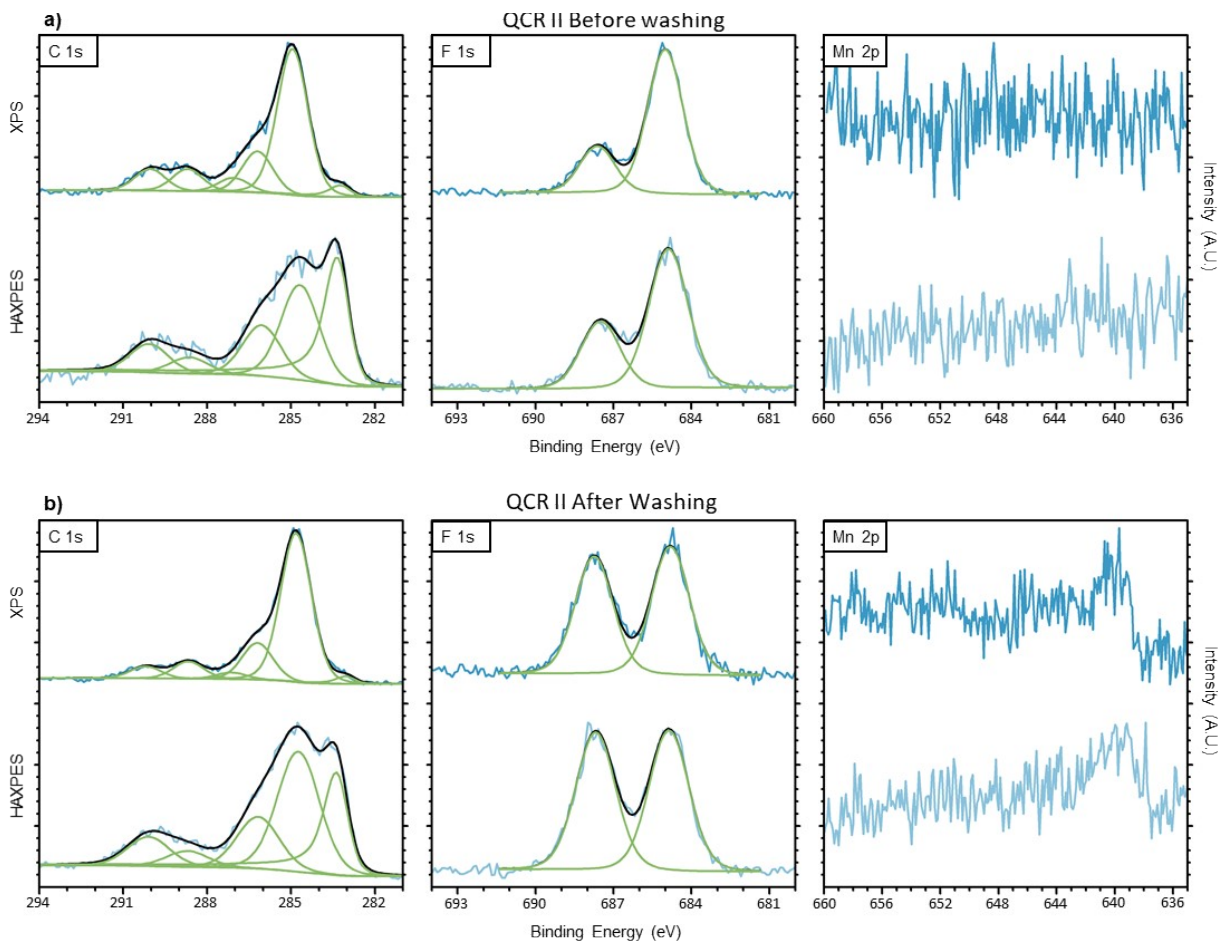


Fig. S2: XPS and HAXPES scans of QCR II a) before and b) after washing with dimethylcarbonate (DMC). Both were scanned before air exposure. Carbon 1s is shown on the left, fluorine 1s in the middle and manganese 2p on the right. XPS scans are displayed above HAXPES scans taken of the same spot. Peak fittings are the same as that given in.

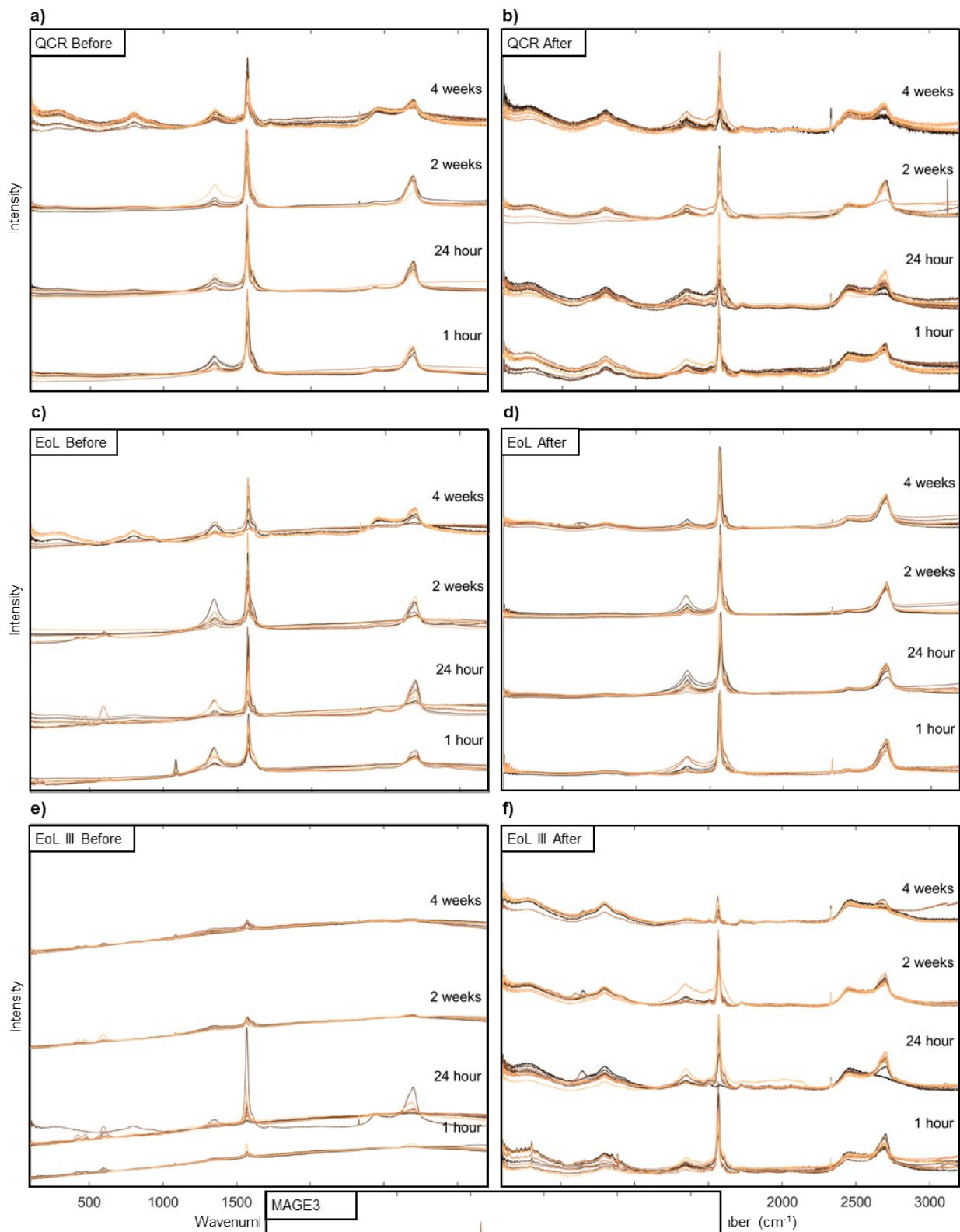
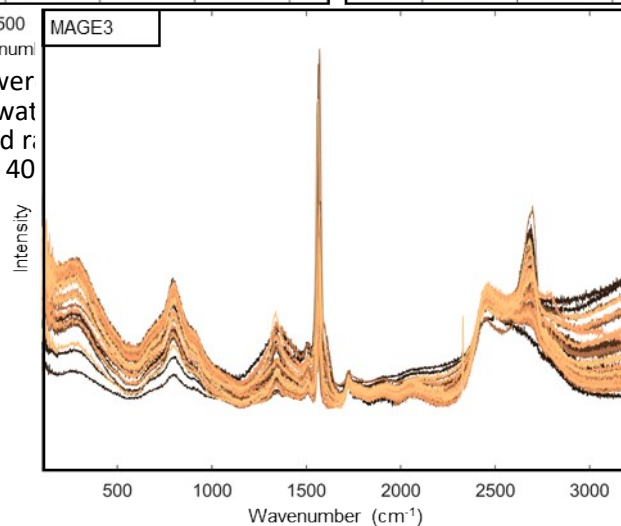


Fig. S3: 10 Raman spectra were taken before water submersion and b) after. c) EoL before water submersion and d) after. The 10 scans were displaced vertically in the figure. This results in 40



40 Raman spectra were taken before water submersion and f) after. The 10 scans are shown overlapping

Fig. S4: 40 randomly dispersed Raman scans taken of a sample of MAGE3 powder.



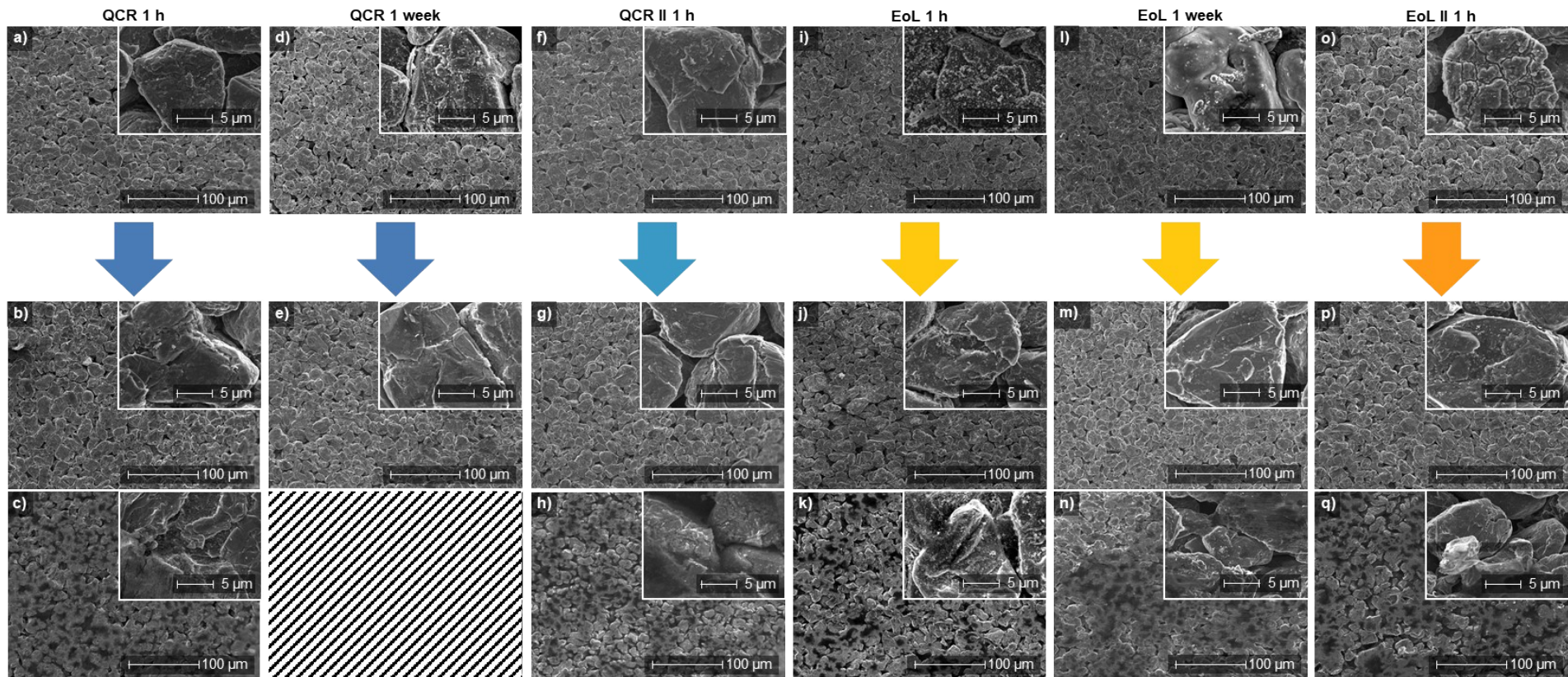


Fig. S5: Large SEM images at 250x magnification with a 5000x magnified SEM image in the top right of each. a) QCR after 1 h of air exposure. b) Water delaminated QCR after 1 h of air exposure, showing the face that originally faced the separator and electrolyte. c) Water delaminated QCR after 1 h of air exposure, showing the face that was attached to the current collector. d-e) Similar to (a-c) however for QCR after 1 week of air exposure for the top image and delamination after 2 weeks for the bottom. An image of the face that was attached to the current collector was not acquired due to difficulties in delamination. f-h) Shows QCR II after 1 h of air exposure and delamination after the same time period. i-k) Shows EoL after 1 h of air exposure and delamination after the same time period. l-n) EoL after 1 week of air exposure and delamination after 2 weeks. o-q) Shows EoL II after 1 h of air exposure and delamination after the same time period.

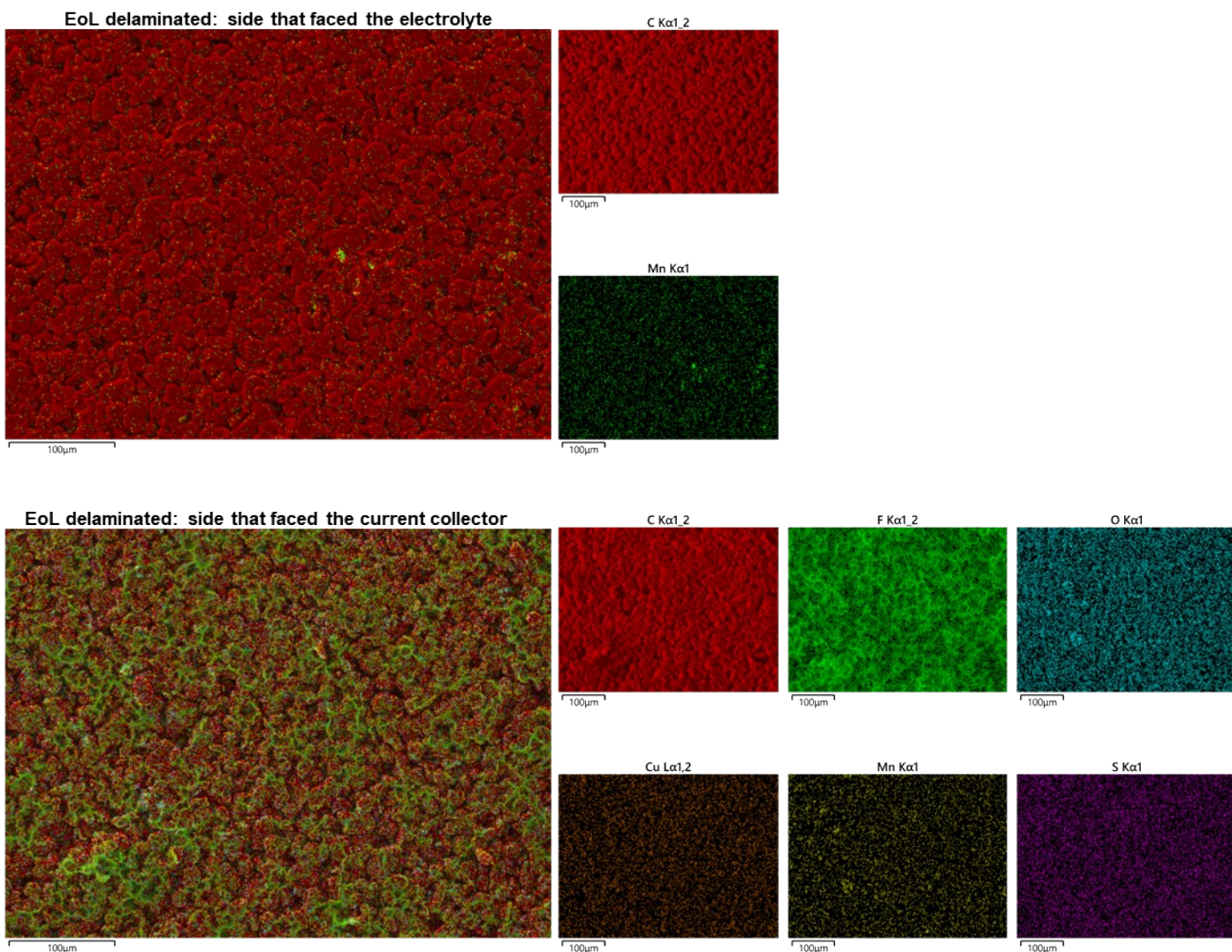


Fig. S6: Elemental mappings were taken using a HITACHI TH4000plus SEM with an energy dispersive X-ray spectroscopy (EDX) detector from AztecOne. The 15 kV backscattered electron mode was used. Shown above are the two sides of anode film from 1 h air-exposed EoL after delamination. The top displays the side that faced the electrolyte and separator, where only carbon and manganese concentrations were enough to be picked up via elemental mapping. The images below shows PVDF binder keeping the graphite together on the side that faced the current collector before the delamination.



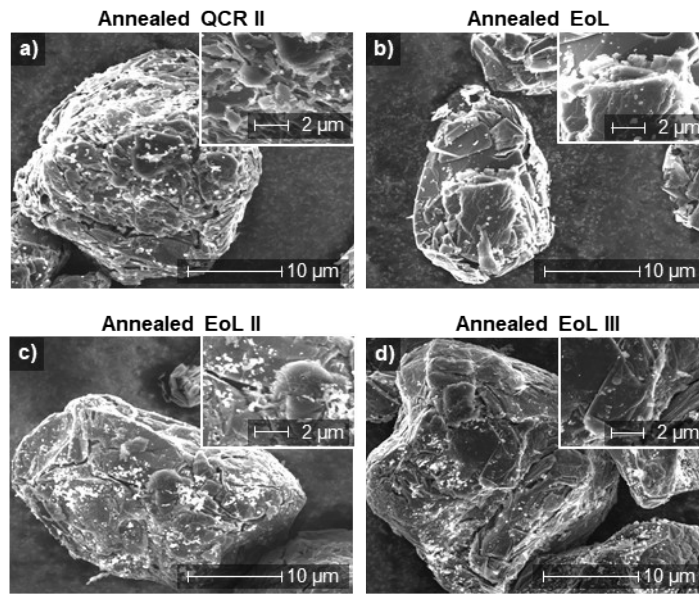
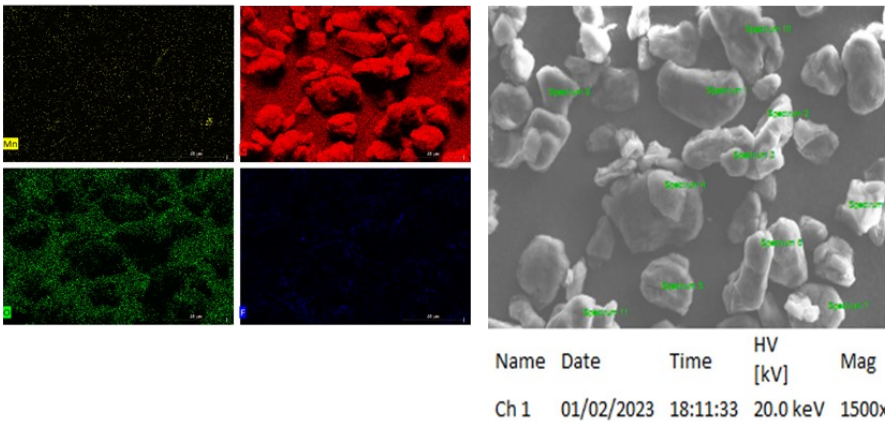


Fig. S7: Large 5000x magnified SEM images with 12000x magnified SEM images in the top right of each. a) QCR II b) EoL c) EoL II d) EoL III delaminated after 2 weeks of air exposure and annealing to 500 °C for 1 h.

EoL III 1 hour annealed



EoL III 2 weeks annealed

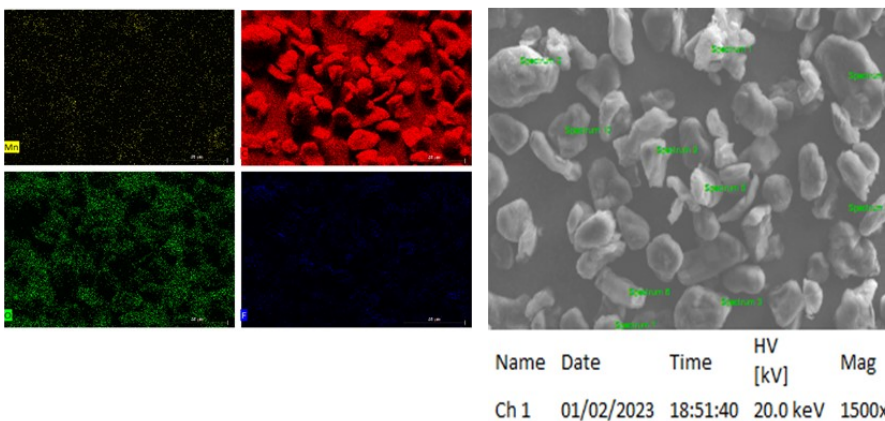


Fig. S8: Elemental mappings were taken using a Zeiss EVO15 VP ESEM with an energy dispersive X-ray spectroscopy detector. 20 kV backscattered electron mode was used. EoL III after 1 hour of air exposure before delamination followed by annealing at 500 °C for 1h hour is shown above and EoL III after 2 weeks of air exposure before delamination followed by the same annealing is shown below.

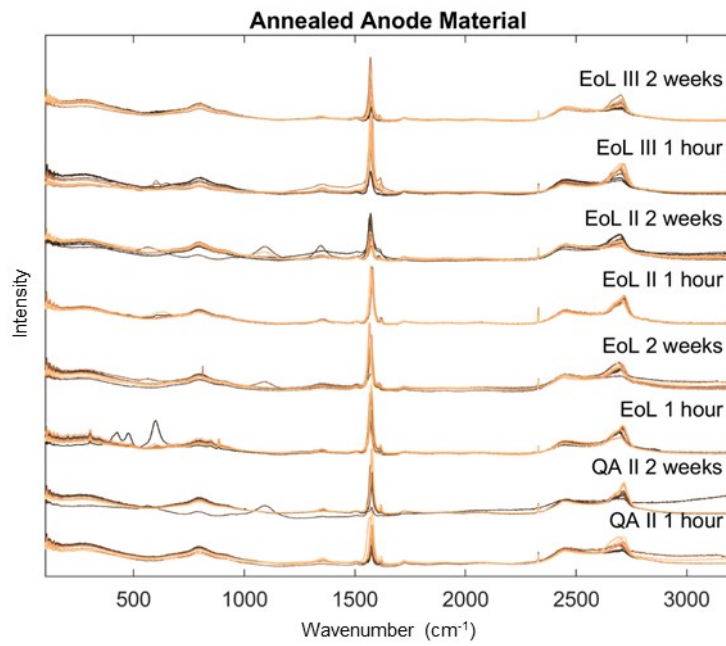


Fig. S9: 10 Raman spectra for each anode film after annealing to 500 °C for 1 h. 1 hour and 2 weeks refers to the time exposed to air before water delamination.

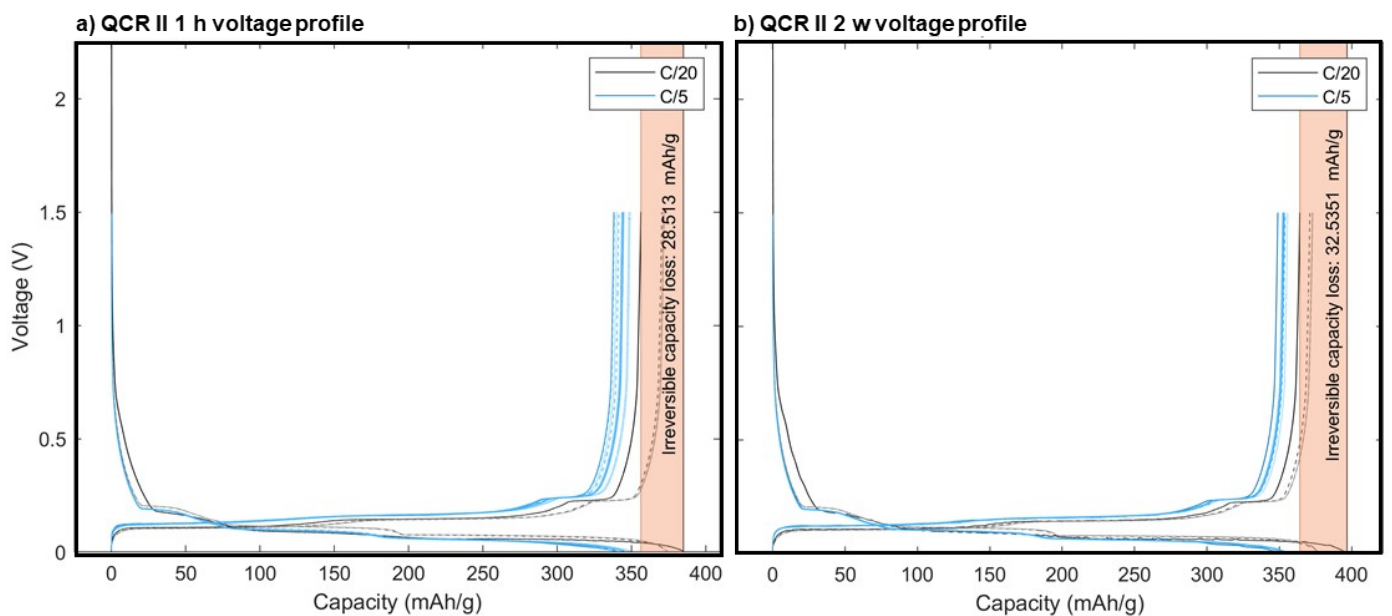


Fig. S10: Voltage profiles of 1 half-cell for both a) QCR II 1 h and b) QCR II 2 w. 20 cycles were conducted with the first 5 represented in black at C/20 and the following 15 in blue at C/5. The solid black line represents the first cycle and the irreversible capacity is represented by the orange block.

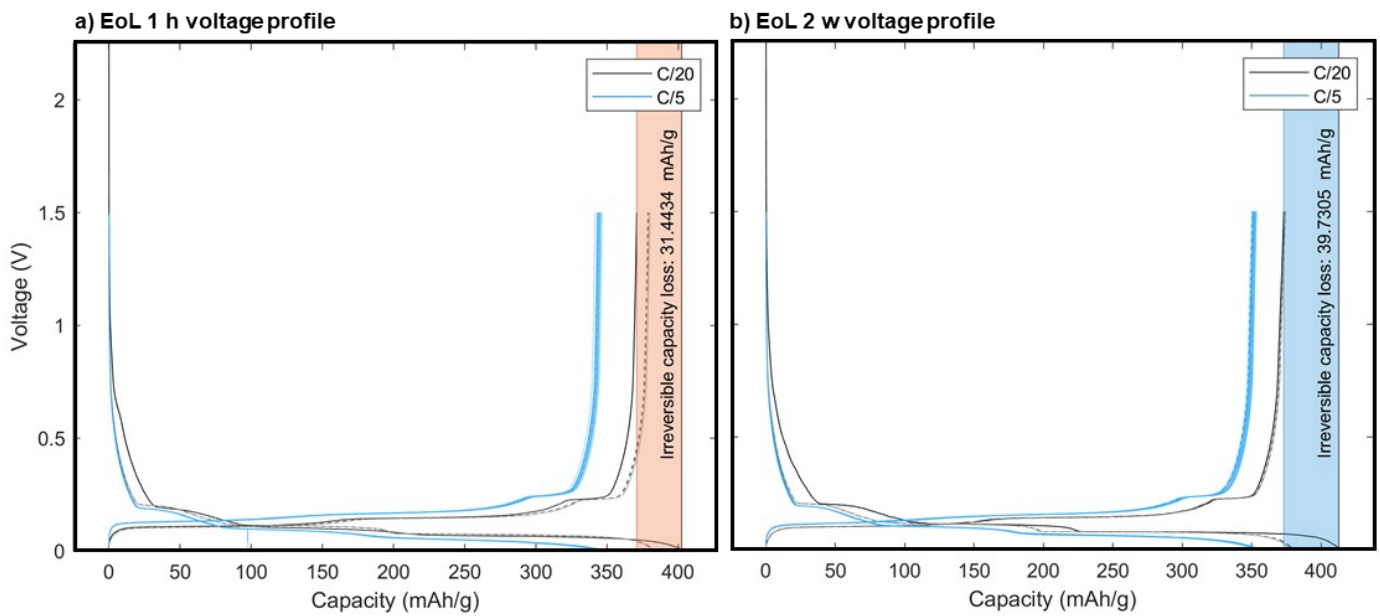


Fig. S11: Voltage profiles of 1 half-cell for both a) EoL 1 h and b) EoL 2 w. 20 cycles were conducted with the first 5 represented in black at C/20 and the following 15 in blue at C/5. The solid black line represents the first cycle and the irreversible capacity is represented by the orange and blue block.

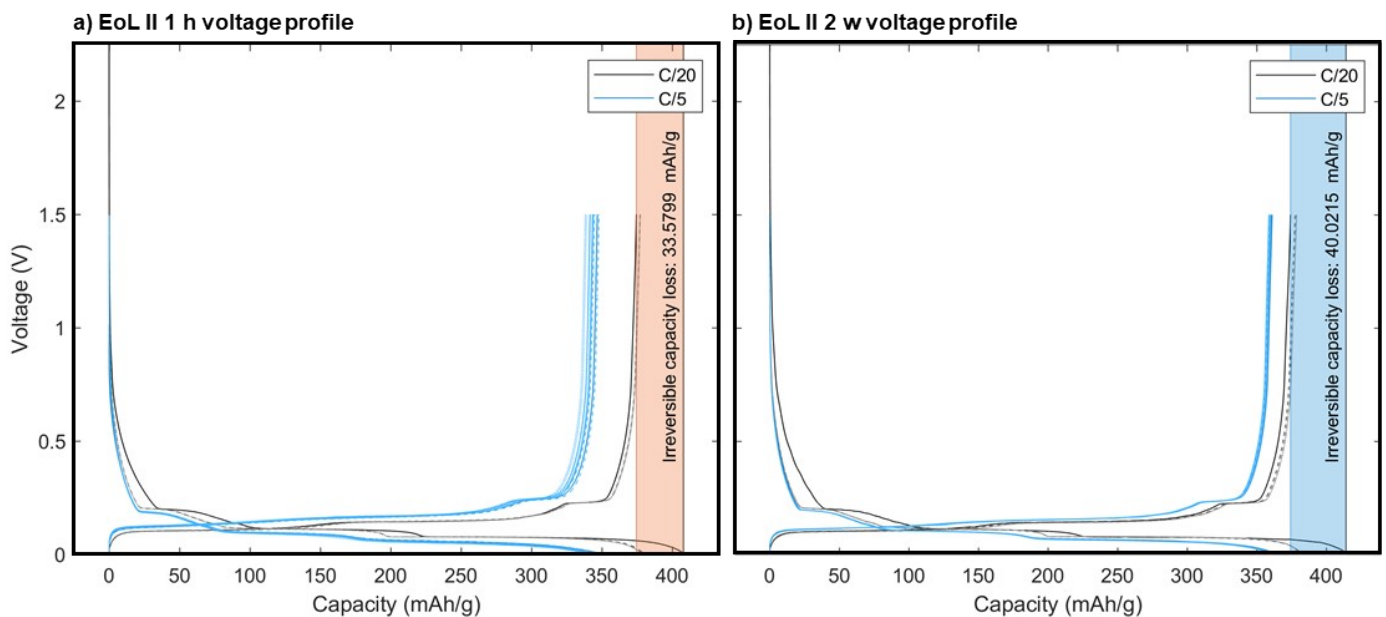


Fig. S12: Voltage profiles of 1 half-cell for both a) EoL II 1 h and b) EoL II 2 w. 20 cycles were conducted with the first 5 represented in black at C/20 and the following 15 in blue at C/5. The solid black line represents the first cycle and the irreversible capacity is represented by the orange block.

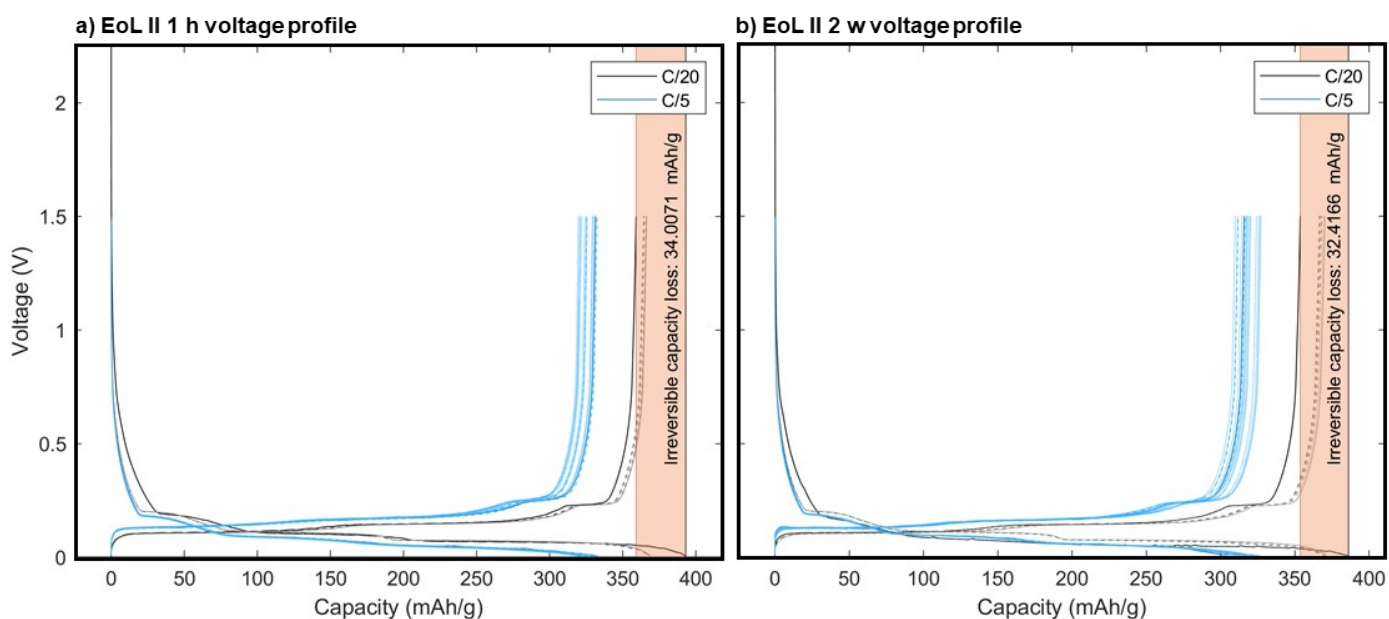


Fig. S13: Voltage profiles of 1 half-cell for both a) EoL III 1 h and b) EoL III 2 w. 20 cycles were conducted with the first 5 represented in black at C/20 and the following 15 in blue at C/5. The solid black line represents the first cycle and the irreversible capacity is represented by the orange block.

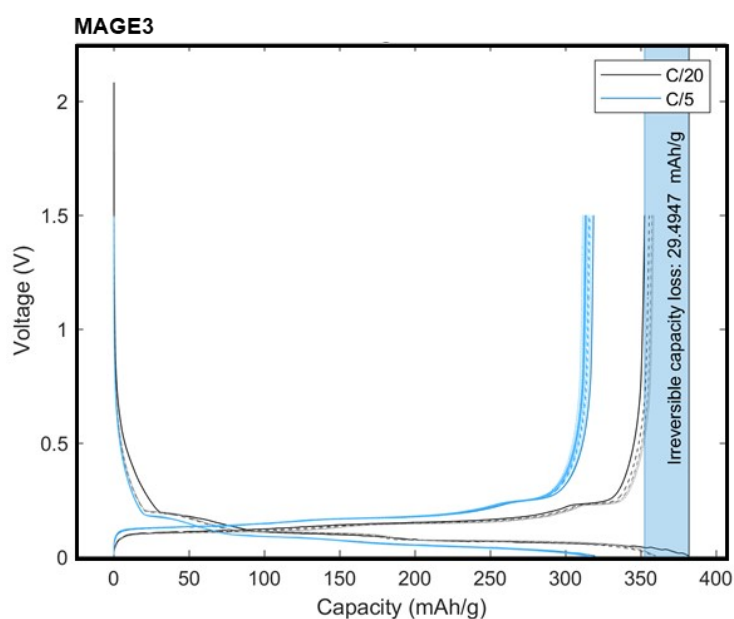


Fig. S14: Voltage profile of 1 half-cell made using MAGE3 graphite. 20 cycles were conducted with the first 5 represented in black at C/20 and the following 15 in blue at C/5. The solid black line represents the first cycle and the irreversible capacity is represented by the blue block.